Accuracy Improvement of Upper Bound Analysis of Bimetallic Rods Extrusion Using a New Velocity Field

H. Afrasiab*
Department of Mechanical Engineering,
Babol Noshirvani University of Technology, Iran
E-mail: afrasiab@nit.ac.ir
*Corresponding author

M. Gasemi-Mahallekolaei
Department of Mechanical Engineering,
Babol Noshirvani University of Technology, Iran
E-mail: mo.ghasemi09@gmail.com

Received: 19 July 2016, Revised: 16 October 2016, Accepted: 23 October 2016

Abstract: In this paper, the direct extrusion process of bimetallic rods in conical dies is analyzed by an improved upper bound method. The deformation zone is subdivided into six smaller zones and by considering a non-spherical entrance boundary to the deformation zone, a velocity field is presented which is different from velocity fields employed in previous studies. The total power consumption of the process including internal, shear and frictional powers is obtained using this velocity field, and then the forming force is calculated by employing the upper bound theory. The superior accuracy of the proposed analysis is demonstrated by comparing the computed force with available experimental data and results of an upper bound analysis in the literature. Finally, the developed model is employed to study the effect of some process parameters on the forming load. It is observed that there is an optimal die angle that minimizes the extrusion force. The value of this optimum angle increases with friction coefficient.

Keywords: Bimetallic rods, Direct extrusion, Upper bound analysis

Reference: Afrasiab, H., Gasemi-Mahallekolaei, M., "Accuracy Improvement of Upper Bound Analysis of Bimetallic Rods Extrusion Using a New Velocity Field", Int J of Advanced Design and Manufacturing Technology, Vol. 9/ No. 4, 2016, pp. 99-107.

Biographical notes: H. Afrasiab received his PhD in Mechanical Engineering from Sharif University of Technology, in 2011. He is currently Assistant Professor at the Department of Mechanical Engineering, Babol University of Technology, Babol, Iran. His current research interest includes finite element modelling of multi-physics problems and analytical study of metal forming processes. **M. G. Mahallekolaei** received his MSc in mechanical Engineering from Babol University of Technology in 2015. Currently, he works as a research assistant in strength of materials laboratory in Babol University of Technology, Iran. His current research focuses on numerical and analytical modelling of metal forming processes.

1 INTRODUCTION

Bimetallic rods consisting of two different metal layers have been used widely in various industries due to their distinct properties such as high electrical conductivity, high corrosion resistivity, high strength, better wear resistance, etc. A hybrid rod made of aluminum and copper is one of the most commonly used types of bimetallic rods. This metal system combines the light weight and easy availability of aluminum with superior conductivity of copper. Consequently, the resulting product offers 40% to 50% reduction in weight and 30% to 40% reduction in price for equivalent conductivity as compared to copper [1]. The extrusion process is considered to be one of the most effective methods for manufacturing bimetallic rods and tubes. The compressive stress state in this process is helpful to produce a suitable metallurgical bond between metal layers [2]. In this process, like all other metal forming methods, the calculation and optimization of the forming force is of primary importance. However, calculation of exact forces to cause plastic deformation is often difficult and consequently, numerous efforts have been made to appropriately estimate the force required to accomplish the involved plastic deformation. One the most popular approaches for force estimation is the upper bound method which always predicts a value higher than the true required force.

A number of studies have used the upper bound approach to analyze the extrusion process. Osakada et al in [3] investigated the extrusion of bimetallic rods in conical dies by experimental and upper bound approaches. The effects of extrusion ratio, die angle and frictional shear stress were considered in their study. Avitzur et al used upper bound method in [4], [5] to derive a criterion for prevention of core fracture during extrusion of bimetal rods. They concluded that the variables affecting core fracture are: reduction in area (r%), die geometry, friction, relative size of core and relative strength of the core. Peng in [6] investigated the geometric shape of the deformation zone in rod extrusion by an upper bound analysis. The boundary at the entrance to the deformation zone was assumed to be an arbitrary curved surface, whilst the boundary at the exit was assumed to be a spherical surface. It was shown that the boundary at the entrance of the deformation zone is generally a concave ellipsoidal surface, the concavity decreases with increasing extrusion ratio and friction factor and decreasing die angle. Tokuno and Ikeda in [7] studied some flow characteristics of deformation in the extrusion of composite rods using the upper-bound approach. They observed that when the core material is softer than the sleeve material, the interface between two materials suppresses effectively the flow of the soft core throughout the deformation zone. On the other hand, when the core is harder than the sleeve, the interface imposes a force to constrain the flow of the outer soft material only in the latter half of the deformation path. Chitkara and Aleem in [8] extended the generalized upper bound technique to analyze the problem of bimetallic tube extrusions through profile shaped dies and mandrel combinations. Theoretical results of mean extrusion pressures obtained from the generalized upper bound analysis were compared with those obtained earlier by the generalized slab method of analysis and some experiments. Hwang and Hwang in [9] proposed a set of stream functions to investigate the plastic deformation behavior of rods during the axisymmetric extrusion of composite rods through a conical die. They determined the radius ratio of the core layer at the exit of the die and the plastic region within the die by using the upper bound method and minimization of the total power. Haghighat and Asgari in [10] used an upper-bound approach to analyze the extrusion process of bimetallic tubes through dies of any shape with moving cylindrical shaped mandrel. A generalized kinematically admissible velocity field was developed to evaluate the internal power and the power dissipated on frictional and velocity discontinuity surfaces and the total power. Haghighat and Amjadian in [11], used an upper bound solution for extrusion of bimetallic rectangular cross-section bars to determine the extrusion pressures for two types of die shapes, namely an optimum wedge shaped die as a linear die profile and an optimum streamlined die shape as a curved die profile. Haghighat and Mahdavi in [12] employed an upper bound approach to analyze the bimetallic rod extrusion process through rotating conical dies. The relative extrusion pressure was evaluated by equating the total power with the external power produced by axial movement of the punch and the power induced by rotation of the die. In another paper [13], they studied bimetal tube extrusion process through rotating conical dies analytically and numerically. By balancing the moment applied by the rotary die with the moments caused by the circumferential frictions in the container and on the mandrel, the twisting length of the material in the container was determined. Haghighat and Shayesteh in [14] analyzed the extrusion process of hybrid sheet metals through arbitrarily curved dies by the method of upper bound. The extrusion forces for two types of die shapes, namely an optimum wedge shaped die and an optimum streamlined die shape for a hybrid sheet composed of copper as sleeve and aluminum as core were determined. A review on previous studies shows that in most upper bound analyses of the bimetallic extrusion, the boundary at the entrance to the deformation zone is assumed to be a spherical surface for the sake of simplicity. For example, this assumption

was employed by Avitzur et al in [4], [5], Tokuno and Ikeda in [7], Haghighat and Asgari in [10], Haghighat and Amjadian in [11], Haghighat and Mahdavi in [12], Haghighat and Shayesteh in [14]. However, some observations suggest that a better choice for the shape of the entrance boundary may improve the results of the upper bound analysis. For instance, Peng in [6] reported that assuming a concave ellipsoidal surface for the boundary at the entrance to the deformation zone increases the upper bound method accuracy in extrusion of single-metal rods. Consequently, in this paper, an ellipsoidal surface is assumed for the entrance boundary to the deformation zone in extrusion of bimetallic rods. Furthermore, in contrast to the analysis performed in [6], the incompressibility condition is also applied to obtain a different velocity field. The detailed analysis is elaborated in the following sections.

2 UPPER BOUND ANALYSIS

Based on the upper bound theory, for a rigid-plastic Von-Misses material and amongst all the kinematically admissible velocity fields, the actual one that minimizes the power required for material deformation is expressed as [11]:

$$J^* = \frac{2}{\sqrt{3}}\sigma_0 \int_V (\frac{1}{2}\dot{\varepsilon}_{ij}\dot{\varepsilon}_{ij})^{1/2}\, dV + \frac{\sigma_0}{\sqrt{3}}\int_{S_v} |\Delta\upsilon|\, dS + m\frac{\sigma_0}{\sqrt{3}}\int_{S_f} \tau\, |\Delta\upsilon|\, dS \quad (1)$$

Where σ_0 is the mean flow stress of the material, ε_{ij} strain rate tensor, m constant friction factor, V volume of plastic deformation zone, S_V and S_f area of velocity discontinuity and frictional surfaces, respectively, and $\Delta\upsilon$ is the amount of velocity discontinuity on the frictional and discontinuity surfaces. Schematic views of the bimetallic extrusion process through a conical die are shown in Figs. 1 and 2. The deformation zone which is divided into six smaller regions and the associated geometrical variables are also presented in these figures. The workpiece is made up two different metals with the mean flow stresses of σ_{0c} and σ_{0s}. The subscripts c and s refer to the core and sleeve materials, respectively. R_f is the outer radius of the sleeve material and R_{cf} is its inner radius both after extruding, where R_i and R_{ci} are the outer and inner radius of the sleeve metal in the initial workpiece. α is the die semi-angle and β is the angle of the boundary between the core and the sleeve. V_i and V_f are the inlet and outlet velocities and the boundaries are denoted by S. Furthermore, it is assumed that the metallurgical bond exists between the core and the sleeve both before and after extruding and slippage does not occur on the core-sleeve interface.

2.1. Velocity fields and strain rate components

In the upper bound analysis, the first step is to choose a kinematically admissible velocity field for the material undergoing plastic deformation. A velocity field is called kinematically admissible if it is derived from incompressibility condition and satisfies the velocity boundary conditions.

For describing the velocity field, a spherical coordinate system (ρ, θ, ϕ) is employed whose origin is located at point O, i.e. the intersection of the die extension with the midline. The material under deformation is divided into six zones, as shown in Fig. 1. The velocity filed is continuous within each region. In zones I_c and I_s, the workpiece is assumed to flow as a rigid body in the extrusion direction. In zones II_c and II_s the material deforms in the die and in zones III_c and III_s it moves as a rigid body and leaves the die. Base on the volume constancy condition, one can write:

$$V_i = \frac{R_f^2}{R_i^2}V_f \quad (2)$$

The boundary of the deformation zone at the exit is assumed to be a spherical surface whose center is located at point O. The radius of this boundary, ρ_f is obtained by the following relation:

$$\rho_f = \frac{R_f}{\sin\alpha} = \frac{R_{cf}}{\sin\beta} \quad (3)$$

The boundary at the entrance to the deformation zone is assumed to an exponential surface with the following relation between r and θ [6]:

$$\rho_i = \frac{R_i}{\sin\alpha}\exp[\frac{b(\theta-\alpha)}{\alpha}] \quad (4)$$

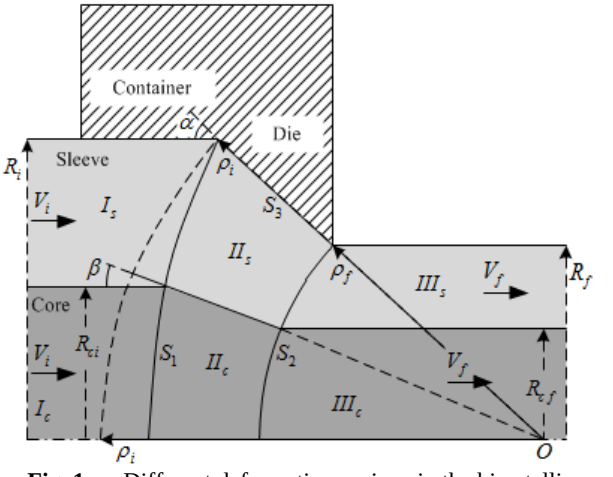

Fig. 1 Different deformation regions in the bimetallic extrusion process through a conical die

Quantity b is a geometric parameter that determines the shape of the boundary. I.e. $b > 0$ relates to a concave

ellipsoidal surface, $b=0$ to a spherical surface and $b<0$ to a convex ellipsoidal surface.

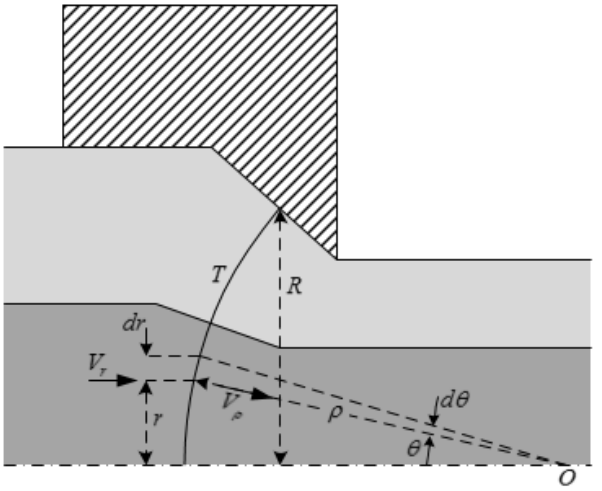

Fig. 2 The geometrical variables in the bimetallic extrusion

The function of the boundary for equal axial components of velocity in the deformation zone may thus be expressed as [6]:

$$\rho(\theta,R)=\frac{R}{\sin\alpha}\exp[\frac{b(\theta-\alpha)}{\alpha}\frac{R-R_f}{R_i-R_f}]=\frac{R}{\sin\alpha}g(\theta,R) \quad (5)$$

Where function g is given by [6]:

$$g(\theta,R)=\exp[\frac{b(\theta-\alpha)}{\alpha}\frac{R-R_f}{R_i-R_f}] \quad (6)$$

In order to determine the material velocity field in the deformation zone, the incompressibility condition of the plastic deformation is imposed. By ignoring the elastic deformation, the incompressibility condition in the spherical coordinates reads [15]:

$$\dot{\varepsilon}_{\rho\rho}+\dot{\varepsilon}_{\theta\theta}+\dot{\varepsilon}_{\phi\phi}=0 \quad (7)$$

This equation is used in the following sections to obtain the velocity field and strain rate components in different deformation regions.

2-1-1 velocity and strain rate in regions I_c and I_s

In regions I_c and I_s, the material has not reached the die entrance, yet. Consequently, no deformation occurs in these regions and the material moves as a rigid body in the die axial direction with constant velocity of V_i. Since the process is axisymmetric, the ϕ component of the velocity is zero. Furthermore, by decomposing the axial velocity vector of the material into ρ and θ directions, the following velocity field is obtained:

$$\begin{aligned} V_\rho &= -V_i\cos\theta \\ V_\theta &= V_i\sin\theta \\ V_\phi &= 0 \end{aligned} \quad (8)$$

In spherical coordinates, the following relations are used to derive the strain rate components from the velocity vector [15]:

$$\begin{aligned} \dot{\varepsilon}_{\rho\rho} &= \frac{\partial V_\rho}{\partial\rho} \\ \dot{\varepsilon}_{\theta\theta} &= \frac{1}{\rho}\frac{\partial V_\theta}{\partial\theta}+\frac{V_\rho}{\rho} \\ \dot{\varepsilon}_{\phi\phi} &= \frac{1}{\rho\sin\theta}\frac{\partial V_\phi}{\partial\phi}+\frac{V_\rho}{\rho}+\frac{V_\theta}{\rho}\cot\theta \\ \dot{\varepsilon}_{\rho\theta} &= \frac{1}{2}(\frac{\partial V_\theta}{\partial\rho}-\frac{V_\theta}{\rho}+\frac{1}{\rho}\frac{\partial V_\rho}{\partial\theta}) \\ \dot{\varepsilon}_{\theta\phi} &= \frac{1}{2}(\frac{1}{\rho\sin\theta}\frac{\partial V_\theta}{\partial\phi}+\frac{1}{\rho}\frac{\partial V_\phi}{\partial\theta}-\frac{\cot\theta}{\rho}V_\phi) \\ \dot{\varepsilon}_{\phi\rho} &= \frac{1}{2}(\frac{\partial V_\phi}{\partial\rho}-\frac{V_\phi}{\rho}+\frac{1}{\rho\sin\theta}\frac{\partial V_\rho}{\partial\phi}) \end{aligned} \quad (9)$$

Applying these relations to Eq. (8) gives:

$$\begin{aligned} \dot{\varepsilon}_{\rho\rho} &= 0 \\ \dot{\varepsilon}_{\theta\theta} &= 0 \\ \dot{\varepsilon}_{\phi\phi} &= 0 \\ \dot{\varepsilon}_{\rho\theta} &= 0 \\ \dot{\varepsilon}_{\theta\phi} &= 0 \\ \dot{\varepsilon}_{\phi\rho} &= 0 \end{aligned} \quad (10)$$

2.1.1. Velocity and strain rate in regions II_c and II_s

In these regions that are surrounded by three velocity discontinuity surfaces S_1, S_2 and S_3, the workpiece deforms and its diameter decreases. The radial velocity component in these regions is obtained by assuming volume flow balance on boundary T (Fig. 2). Equating the material volume on two sides of this boundary gives:

$$V_r(2\pi r)(dr)=-V_\rho(2\pi\rho)(\rho\,d\theta\sin\theta) \quad (11)$$

On the other hand, according to Fig. 2, the following relation holds between r and ρ:

$$r=\rho\sin\theta \quad (12)$$

Substituting from Eq. (12) back into Eq. (11) and considering Eqs. (2) and (5) yields:

$$V_\rho=-V_i\left(\frac{R_i}{R}\right)^2\left(\frac{b}{\alpha}\frac{R-R_f}{R_i-R_f}\sin\theta+\cos\theta\right) \quad (13)$$

The axial symmetry assumption in this region gives:

$$V_\phi = 0 \tag{14}$$

Now substituting from Eqs. (13) and (14) into Eq. (9) and using Eq. (7) results the following relation for V_θ:

$$V_\theta = V_i \frac{\rho_i^2 \sin\alpha}{R}\frac{\partial g}{\partial \rho} \tag{15}$$

Where:

$$\frac{\partial g}{\partial \rho} = \frac{\partial g}{\partial R}\frac{\partial R}{\partial \rho} = \frac{b(\theta-\alpha)}{\alpha}\frac{\sin\alpha}{\gamma(R_i - R_f)} \tag{16}$$
$$\gamma = \left(1 + \frac{b(\theta-\alpha)}{\alpha}\frac{R}{R_i - R_f}\right)$$

The strain rate components are also obtained as follows:

$$\dot{\varepsilon}_{\rho\rho} = -V_i \frac{{\rho_i}^2 \sin^2\alpha}{\rho^3}\frac{1}{g^2}[2(R\frac{\partial g}{\partial \rho} - \sin\alpha)g\cos\theta$$
$$+(-2\frac{\partial g}{\partial \theta}\sin\alpha + R\frac{\partial g}{\partial \rho}\frac{\partial g}{\partial \theta} + gR\frac{\partial^2 g}{\partial \rho \partial \theta})\sin\theta]$$
$$\dot{\varepsilon}_{\theta\theta} = V_i(\frac{\rho_i \sin\alpha}{R})^2\frac{1}{g}[(\frac{\partial^2 g}{\partial \rho \partial \theta} - \frac{1}{g}\frac{\partial g}{\partial \theta})\sin\theta$$
$$+(\frac{\partial g}{\partial \rho} - \frac{\sin\alpha}{R})\cos\theta]$$
$$\dot{\varepsilon}_{\phi\phi} = V_i(\frac{\rho_i \sin\alpha}{R})^2\frac{1}{g}[(\frac{\partial g}{\partial \rho} - \frac{\sin\alpha}{R})\cos\theta + \frac{1}{g}\frac{\partial g}{\partial \theta}\sin\theta]$$
$$\dot{\varepsilon}_{r\theta} = \frac{1}{2}V_i(\frac{\rho_i \sin\alpha}{R})^2\frac{1}{g}\{[-2\frac{\partial g}{\partial \rho} + \frac{R}{\sin\alpha}(\frac{\partial g}{\partial \rho})^2 + \frac{R}{\sin\alpha}g\frac{\partial^2 g}{\partial \rho^2}$$
$$+\frac{\sin\alpha}{R}[-1 - \frac{1}{g^2}(\frac{\partial g}{\partial \theta})^2 + \frac{1}{g}\frac{\partial^2 g}{\partial \theta^2}]]\sin\theta$$
$$+\frac{\sin\alpha}{R}\frac{1}{g}\frac{\partial g}{\partial \theta}\cos\theta\}$$
$$\dot{\varepsilon}_{\theta\phi} = 0$$
$$\dot{\varepsilon}_{\phi r} = 0$$
(17)

2.1.2. Velocity and strain rate in III_c and III_s

In III_c and III_s regions, the material deformed in region *II* leaves the die exit (S_2) with constant velocity of V_f in the axial direction. The material moves as a rigid body in this region and no deformation occurs. Due to axial symmetry, the velocity component in the φ direction is zero and other components are obtained as:

$$V_\rho = -V_f\cos\theta$$
$$V_\theta = V_f\sin\theta \tag{18}$$
$$V_\phi = 0$$

Replacing Eq. (18) into Eq. (9), the following equations are derived for strain rate components:

$$\dot{\varepsilon}_{\rho\rho} = 0$$
$$\dot{\varepsilon}_{\theta\theta} = 0$$
$$\dot{\varepsilon}_{\phi\phi} = 0$$
$$\dot{\varepsilon}_{\rho\theta} = 0 \tag{19}$$
$$\dot{\varepsilon}_{\theta\phi} = 0$$
$$\dot{\varepsilon}_{\phi\rho} = 0$$

The results presented in Eqs. (10) and (19) are logical since in regions I_c, I_s, III_c and III_s, the material moves as a rigid body and consequently strain and strain rate components are identically zero. The angle of the interface surface between the sleeve and core materials denoted by β in Fig. (1) is obtained by the following relation:

$$\beta = \sin^{-1}(\frac{R_{ci}}{R_i}\sin\alpha) \tag{20}$$

2.2. Calculation of power components and the forming force

The total power required for performing the extrusion process is made up three parts:

- Internal power of deformation
- The shear power dissipated on velocity discontinuity surfaces
- The frictional power dissipated on the interface between workpiece and die

Consequently, according to Fig. 1, the total power in the presented process is obtained by summing the internal power of deformation in regions II_c and II_s, the energy dissipated on velocity discontinuity surfaces S_1 and S_2, and the frictional dissipated energy on the die surface S_3.

2.2.1. The internal power

The internal power consumed in the deformation zone is given by [15]:

$$\dot{W}_i = \frac{2}{\sqrt{3}}\sigma_0\int_V\sqrt{\frac{1}{2}\dot{\varepsilon}_{ij}\dot{\varepsilon}_{ij}}\,dV \tag{21}$$

Where dV, the volume element in the deformation zone, is obtained as [6]:

$$dV = \left(\frac{R}{\sin\alpha}\right)^2 g^2(1 + \frac{b(\theta-\alpha)}{\alpha(R_i - R_f)}R)\sin\theta\,d\theta\,d\rho dR \tag{22}$$

Since the strain rate components are identically zero in regions *I* and *III*, the internal power is zero in these regions as confirmed by Eq. (21). The internal power consumed by the sleeve is:

$$\dot{W}_{is} = \frac{4\pi}{\sqrt{3}}\sigma_{0s}\int_{\rho_f}^{\rho_i}\int_{\beta}^{\alpha}\sqrt{\frac{3}{4}\dot{\varepsilon}_{\rho\rho}^2\dot{\varepsilon}_{\rho\theta}^2}\,\frac{R^2}{\sin^2\alpha}\,g^2(g + \frac{R}{\sin\alpha}\frac{\partial g}{\partial\rho})\sin\theta\,\mathrm{d}\theta\,\mathrm{d}\rho \quad (23)$$

Where σ_{0s} is the mean flow stress of the sleeve material:

$$\sigma_{0s} = \frac{\int_0^{\varepsilon}\sigma_s\,\mathrm{d}\varepsilon}{\varepsilon} \quad , \qquad \varepsilon = \ln\frac{R_i^2 - R_{ci}^2}{R_f^2 - R_{cf}^2} \quad (24)$$

The internal power for the core material is calculated similarly:

$$\dot{W}_{ic} = \frac{4\pi}{\sqrt{3}}\sigma_{0c}\int_{\rho_f}^{\rho_i}\int_{0}^{\beta}\sqrt{\frac{3}{4}\dot{\varepsilon}_{\rho\rho}^2\dot{\varepsilon}_{\rho\theta}^2}\,\frac{R}{\sin^2\alpha}^2\,g^2(g + R\frac{\partial g}{\partial R})\sin\theta\,\mathrm{d}\theta\,\mathrm{d}\rho \quad (25)$$

Where σ_{0c} is the mean flow stress of the core material:

$$\sigma_{0c} = \frac{\int_0^{\varepsilon}\sigma_c\,\mathrm{d}\varepsilon}{\varepsilon} \quad , \qquad \varepsilon = \ln\frac{R_{ci}^2}{R_{cf}^2} \quad (26)$$

The overall internal power in region *II* is calculated by summing the internal power of the sleeve and core materials:

$$\dot{W}_i = \dot{W}_{ic} + \dot{W}_{is} \quad (27)$$

2.2.2. The shear power

The equation for the power losses along the shear surface of velocity discontinuity is:

$$\dot{W}_S = \frac{\sigma_0}{\sqrt{3}}\int_{S_v}|\Delta\upsilon|\,\mathrm{d}S \quad (28)$$

Where the velocity discontinuity and the area element for surface S_1 and S_2 are [6]:

$$|\Delta\upsilon_1| = V_i\sqrt{1+(\frac{b}{\alpha})^2}\,(1-\rho_i\frac{\partial g}{\partial\rho}|_{R=R_i})\sin\theta \quad (29)$$

$$dS_1 = 2\pi\rho_i^2 g^2(\theta, R_i)\sqrt{1+(\frac{b}{\alpha})^2}\,\sin\theta\,d\theta \quad (30)$$

$$|\Delta\upsilon_2| = V_f\,(1-\rho_f\frac{\partial g}{\partial\rho}|_{R=R_f})\sin\theta \quad (31)$$

$$dS_2 = 2\pi(\rho_f\,\sin\theta)\rho_f\,d\theta \quad (32)$$

The shear power loss along the shear boundary S_1 includes two parts: the power loss in the core $\dot{W}_{S1c}$, and the power loss in the sleeve $\dot{W}_{S1s}$:

$$\dot{W}_{S_{1C}} = \frac{2\pi}{\sqrt{3}}\,\sigma_{oc}\,\rho_i^2 V_i\,[1+(\frac{b}{\alpha})^2] \times\int_0^{\beta}(1-\rho_i\frac{\partial g}{\partial\rho}|_{R=R_i})\,g^2(\theta,R_i)\sin\theta\,\mathrm{d}\theta \quad (33)$$

$$\dot{W}_{S_{1S}} = \frac{2\pi}{\sqrt{3}}\,\sigma_{os}\,\rho_i^2 V_i\,[1+(\frac{b}{\alpha})^2] \times\int_{\beta}^{\alpha}(1-\rho_i\frac{\partial g}{\partial\rho}|_{R=R_i})\,g^2(\theta,R_i)\sin\theta\,\mathrm{d}\theta \quad (34)$$

Similarly the shear power along S_2 is divided into two parts:

$$\dot{W}_{S_{2C}} = \frac{2\pi}{\sqrt{3}}\,\sigma_{0c}\,\rho_f^2 V_f\int_0^{\beta}(1-\rho_f\frac{\partial g}{\partial\rho}|_{R=R_f})\sin^2\theta\,\mathrm{d}\theta \quad (35)$$

$$\dot{W}_{S_{2S}} = \frac{2\pi}{\sqrt{3}}\,\sigma_{0s}\,\rho_f^2 V_f\int_{\beta}^{\alpha}(1-\rho_f\frac{\partial g}{\partial\rho}|_{R=R_f})\sin^2\theta\,\mathrm{d}\theta \quad (36)$$

The total shear power is then [11]:

$$\dot{W}_S = \dot{W}_{S_{1C}} + \dot{W}_{S_{2C}} + \dot{W}_{S_{1S}} + \dot{W}_{S_{2S}} \quad (37)$$

2.2.3. Frictional power

The frictional power dissipated on frictional boundaries is obtained by [16]:

$$\dot{W}_f = m\frac{\sigma_{0s}}{\sqrt{3}}\int_{S_f}|\Delta\upsilon|\,dS \quad (38)$$

The following equations give the velocity discontinuity and the element area for frictional boundary S_3 [6]:

$$|\Delta\upsilon_3| = V_i\,(\frac{R_i}{R})^2(\cos\alpha + \frac{b}{\alpha}\frac{R-R_f}{R_i-R_f}\sin\alpha) \quad (39)$$

$$dS_3 = \frac{2\pi R dR}{\sin\alpha} \quad (40)$$

Substituting from Eqs. (39) and (40) into Eq. (38) gives the frictional power dissipated on the workpiece-die interface:

$$\dot{W}_f = \frac{2\pi}{\sqrt{3}}\,m\sigma_0 V_i\,\rho_i^2 \times\int_{R_f}^{R_i}(\cos\alpha + \frac{b}{\alpha}\frac{R-R_f}{R_i-R_f}\sin\alpha)\,\mathrm{d}R \quad (41)$$

It is to be noted that no slippage and accordingly no friction loss occurs on the common surface between the sleeve and core material. Finally, based on the analysis performed in [16], [17], for avoiding central cracking in rod extrusion, the following relation must be satisfied:

$$b \le \ln \frac{R_i}{R_f} \tag{42}$$

Considering this equation and noting that b is normally a positive value for the entrance boundary [6], in this study the following value is assumed for b:

$$b = 0.5 \ln \frac{R_i}{R_f} \tag{43}$$

2.2.4. The forming force

In extrusion process, the external power, i.e. the power supplied by external forces, is equal to:

$$\dot{W}_T = F_e V_i \tag{45}$$

Where F_e is the required forming force. In the upper-bound approach, the extrusion force is determined by equating the total power with the external power [11]:

$$F_e = \frac{\dot{W}_{is} + \dot{W}_{ic} + \dot{W}_{S_{1S}} + \dot{W}_{S_{2S}} + \dot{W}_{S_{1C}} + \dot{W}_{S_{2C}} + \dot{W}_f}{V_i} \tag{45}$$

Solving this equation gives the force required for performing the bimetallic extrusion process. For this purpose, a Maple program is developed in this study. The solution results are presented in the next section.

3 RESULTS AND DISCUSSION

In order to verify the validity of the preceding analysis, the solution of the upper-bound analysis for a bimetallic extrusion process in a conical die was compared with experimental and upper-bound results presented in [9]. The work-piece dimensions are given in table 1.

Table 1 The workpiece and die dimensions.

Parameter	Value
Core radius (mm)	9
sleeve outer radius (mm)	15
core and sleeve length (mm)	60
die angle	15°
area reduction ratio	0.25

The core and sleeve metals are Aluminum and Copper, respectively. The exponential stress-strain relationships, $\sigma_{Al}=189.2\varepsilon^{0.239}$ Mpa and $\sigma_{cu}=335.2\varepsilon^{0.113}$ Mpa are used for characterizing their deformation in the plastic region. The sticking model with constant friction factor of m=0.2 is employed for describing the friction condition between the sleeve and the die surfaces. The results are compared in Fig. 3. It can be seen that the proposed upper-bound analysis is in good agreement with experimental data. Furthermore, it has higher accuracy than the upper-bound approach presented in [9].

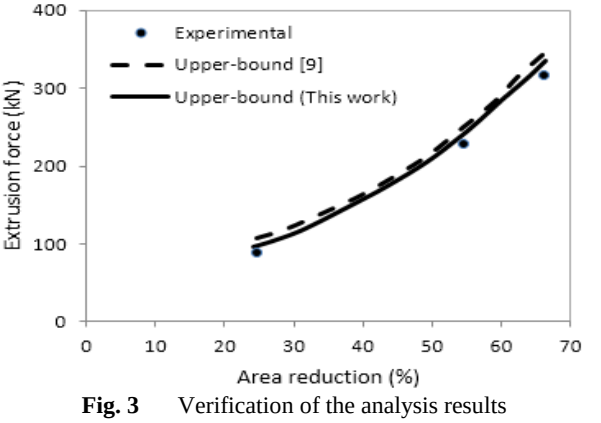

Fig. 3 Verification of the analysis results

The variation of the extrusion force with the die semi-angle is shown in Fig. 4. According to this figure, there is an optimum die angle (approximately 12° in this case) that minimizes the forming force. This observation can be explained by the fact that the contact area between the die and the workpiece and consequently the frictional power loss decreases with increasing the die angle. However, in higher die angles, the shear power loss on velocity discontinuity surfaces increases.

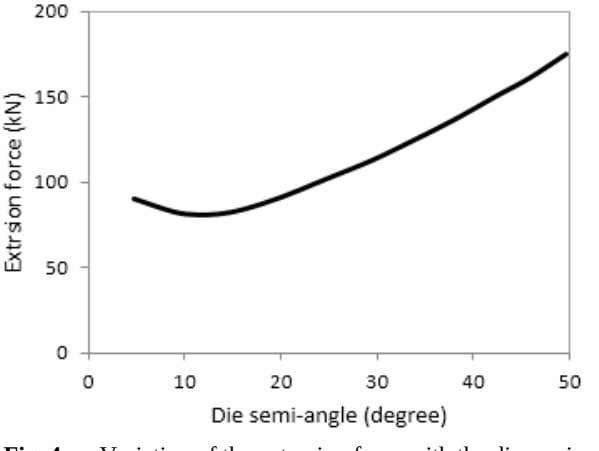

Fig. 4 Variation of the extrusion force with the die semi-angle

Consequently, for each forming condition, there is an optimum die angle for which the total power and accordingly the forming force is a minimum. This interpretation is also confirmed by Fig. 5 which shows

the forming force variation with die angle in different values of friction coefficient. Based on this figure, the optimum die angle increases with increasing friction coefficient. This is due to the fact that by increasing the friction coefficient, the friction power loss makes a more significant contribution in the total power of the process. Therefore, the optimum die angle tends to higher angles where the frictional power decreases.

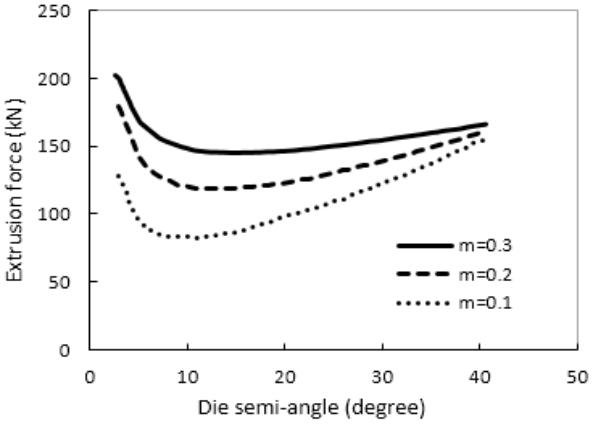

Fig. 5 Variation of the extrusion force in different friction coefficients

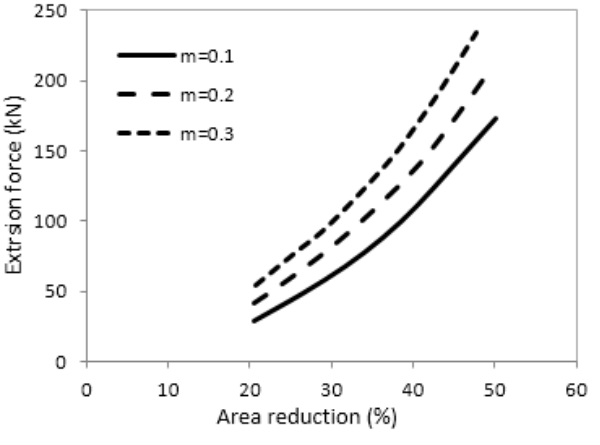

Fig. 6 Comparison of extrusion force in different values of area reduction

The variation of the extrusion force with area reduction percentage is presented in Fig. 6. It can be seen that the extrusion force increases with increasing the area reduction. This stems from the fact that by increasing the area reduction the material undergoes larger deformation which leads to increase of the internal power of deformation and accordingly the total power and the extrusion force.

4 CONCLUSION

In this paper, the extrusion process of bimetallic rods was analyzed by an improved upper-bound approach. A novel velocity field was developed for this purpose. The results were compared with available experimental data and good agreement was found. It was demonstrated that using the exponential function for the shape of the entrance boundary to the deformation zone improves the accuracy of the upper-bound analysis in comparison to the spherical function used in previous studies. Furthermore, it was observed that there is an optimal die angle that minimizes the extrusion force. The value of this optimum angle increases with friction coefficient.

5 NOMENCLATURE

σ_0	mean flow stress of the material
ε_{ij}	strain rate tensor
m	constant friction factor
V	volume of plastic deformation zone
S_V	area of velocity discontinuity
S_f	area of frictional surfaces
Δv	velocity discontinuity
R_f	outer radius of sleeve material after extrusion
R_{cf}	inner radius of sleeve material after extrusion
R_i	outer radius of sleeve metal before extrusion
R_{ci}	inner radius of sleeve metal before extrusion
α	die semi-angle
β	angle of boundary between core and sleeve
V_i	inlet velocity
V_f	outlet velocity
ρ,θ,ϕ	spherical coordinates
b	parameter determining the shape of boundary
S_1,S_2,S_3	velocity discontinuity surfaces

REFERENCES

[1] Ahmed, N., "Extrusion of copper clad aluminum wire," J. Mech. Work Tech., Vol. 2, 1978, pp. 19-32.

[2] Berski, S., Dyja, H., Banaszek, G., and Janik, M., "Theoretical analysis of bimetallic rod extrusion process in double reduction die," Journal of Materials Processing Technology, Vol. 154, 2004, pp. 583–588.

[3] Osakada, K., Limb, M., and Mellor, P. B., "Hydrostatic extrusion of composite rods with hart cores," International Journal of Mechanical Sciences, Vol. 15, 1973, pp. 291-307.
[4] Avitzure, B., Wu, R., Talbert, S., and Chou, Y. T., "Criterion for prevention of core fracture during extrusion of bimetal rods," J. Eng. Ind., Vol. 104, 1982, pp. 293-304.
[5] Avitzure, B., Wu, R., Talbert, S., and Chou, Y. T., "Analysis of core fracture in drawing of bimetal rods and wires," J. Eng. Ind., Vol. 108, 1986, pp. 133-140.
[6] Peng, D. S., "An Upper-bound analysis of the geometric shape of the deformation zone in rod extrusion," Journal of Materials Processing Technology, Vol. 21, 1989, pp. 303-311.
[7] Tokuno, H., and Ikeda, K., "Analysis of deformation in extrusion of composite rods," Journal of Materials Processing Technology, Vol. 26, 1991, pp. 323-335.
[8] Chitkara, N. R., Aleem, A., "Extrusion of axi-symmetric Bimetallic Tubes from Solid Circular Billets: Application of a Generalized upper Bound Analysis and some Experiments," International Journal of Mechanical Sciences, Vol. 43, 2001, pp. 2833-2856.
[9] Hwang, Y. M., and Hwang, T. F., "An Investigation into the Plastic Deformation Behavior With in a Conical Die during Composite Rod Extrusion," J. Mater process Technol., Vol. 121, 2002, pp. 226-233.
[10] Haghighat, H., Asgari, G. R., "A generalized spherical velocity field for bimetallic tube extrusion through dies of any shape," International Journal of Mechanical Sciences, Vol. 53, 2011, pp. 248-253.
[11] Haghighat, H., Amjadian, P., "A Generalized upper bound solution for Extrusion of bi-metallic Rectangular cross-section bars through dies of any shape," Journal of Theoretical and Applied Mechanics, Vol. 51, 2013, pp. 105-116.
[12] Haghighat, H., Mahdavi, M., "Upper bound analysis of bimetallic rod extrusion process through rotating conical dies," Journal of Theoretical and Applied Mechanics, Vol. 51, 2013, pp. 627-637.
[13] Haghighat, H., Mahdavi, M. M., "Analysis and FEM simulation of extrusion process of bimetal tubes through rotating conical dies," Transactions of Nonferrous Metals Society of China, Vol. 23, 2013, pp. 3392-3399.
[14] Haghighat, H., Shayesteh, H., "Upper bound analysis for hybrid sheet metals extrusion process through curved dies," Transactions of Nonferrous Metals Society of China, Vol. 24, 2014, pp. 3285–3292.
[15] Prager, W., Hodge, P. G., "Theory of Perfectly Plastic Solids", John Wiley and Sons Inc., New York, 1951.
[16] Unckel, H. A., "Extrusion - some experimental work on hot short alloys," Met. Ind., Vol. 49, 1946, pp. 429.
[17] Kalpakjian, S., "Manufacturing Processes for Engineering Materials", 5th ed., Addison-Wesley, Reading, 1984.